# Towards clinical application of RayStretch for heterogeneity corrections in LDR permanent I-125 prostate brachytherapy

*Published online: https://doi.org/10.1016/j.brachy.2017.02.005*

**Fernando Hueso-González[1, 5], Facundo Ballester[2], Jose Perez-Calatayud[2], Frank-André Siebert[3] and Javier Vijande[2, 4, *].**

[1] *Target Systemelektronik GmbH, Heinz-Fangman-Straße 4, 42287 Wuppertal, Germany*
[2] *Unidad Mixta de Investigación en Radiofísica e Instrumentación Nuclear en Medicina (IRIMED), Instituto de Investigación Sanitaria La Fe (IIS-La Fe)-Universitat de Valencia (UV), Valencia, Spain*
[3] *UK S-H, Campus Kiel, Klinik für Strahlentherapie (Radioonkologie), Arnold-Heller-Str. 3, Haus 50, D-24105 Kiel, Germany*
[4] *IFIC (UV-CSIC), E-46100 Valencia, Spain*
[5] *Now with Department of Radiation Oncology, Harvard Medical School and Massachusetts General Hospital, Boston, MA 02114, USA*

* Email: Javier.Vijande@uv.es

**Abstract:**

*Purpose.* RayStretch is a simple algorithm proposed for heterogeneity corrections in low dose rate brachytherapy. It is built on top of TG-43 consensus data and it has been validated with Monte Carlo simulations. In this study, we take a real clinical prostate implant with seventy-one $^{125}$I seeds as reference and we apply RayStretch to analyze its performance in worst-case scenarios.

*Methods and Materials.* To do so, we design two cases where large calcifications are located in the prostate lobules. RayStretch resilience under various calcification density values is also explored. Comparisons against Monte Carlo calculations are performed.

*Results.* Dose-Volume Histogram related parameters like prostate $D_{90}$, rectum $D_{2cc}$, or urethra $D_{10}$ obtained with RayStretch agree within a few percent with the detailed Monte Carlo results for all cases considered.

*Conclusions.* The robustness and compatibility of RayStretch with commercial treatment planning systems indicate its applicability in clinical practice for dosimetric corrections in prostate calcifications. Its use during intraoperative ultrasound planning is foreseen.

**Keywords:** brachytherapy, low dose rate, heterogeneities, prostate, calcifications, dosimetry.

**PACS numbers:** 87.53.Jw, 87.55.K, 87.53.Kn, 87.55.-x, 87.55.Gh, 87.53.Bn, 87.19.X-, 87.59.bd

## Introduction

Permanent seed implants have become a common brachytherapy (BT) treatment for patients with low-risk prostate cancer [1] [2]. This medical technique involves the permanent placement of radioactive seeds in the prostate under ultrasound (US) guidance. The American Association of Physicists in Medicine (AAPM) task group No. 186 (TG-186), has recently emphasized the importance of properly incorporating tissue density and composition in a consistent manner [3]. This is more relevant in the case of low energy seeds, like the ones containing $^{125}$I, $^{103}$Pd, or $^{131}$Cs used in permanent BT implants. State-of-the-art Treatment Planning Systems (TPS) are able nowadays to take heterogeneities into account, in particular calcifications (accumulation of calcium within the prostate and therefore not water-equivalent), although only for high dose rate (HDR) $^{192}$Ir sources (see ref. [4] and references therein) and based on computed tomography (CT). The presence of such calcifications is a normal occurrence in males >50 years old [5].

Few clinical solutions exist that are able to fully, or partially, incorporate the dosimetric effect of calcifications in prostate BT implants in low-dose-rate (LDR) brachytherapy. Among them, Chibani and Williamson [6] proved for a $^{103}$Pd seed model using a dedicated Monte Carlo (MC) method that calcifications covering 1% – 5% of the prostate volume can reduce the value of $D_{90}$ up to 37%.

Taylor et al. [7] implemented a MC-based solution by developing a dedicated fast MC code, BrachyDose. For its application in clinical practice, including interseed attenuation and the presence of heterogeneities, BrachyDose forces every history to be recycled for all sources. Sutherland et al. [8] investigated the use of various breast tissue segmentation models including the presence of calcifications using BrachyDose for low-energy brachytherapy. Sutherland et al. [9] discussed various calcification modeling schemes for a LDR prostate brachytherapy patient using BrachyDose, highlighting the importance of detailed and accurate calcification modelling.

An initiative to address the presence of calcifications was developed by Mashouf et al. [10]. In this work, inhomogeneity corrections factors (ICF) were derived for the case of $^{103}$Pd breast BT. The agreement between MC simulations and the ICF method remained within 5% in soft tissues up to several centimetres from a $^{103}$Pd seed. In another publication, Mashouf et al. [11] expanded that study to make use of dual energy CT images to extract the ICF in a phantom. The results were also compared to experimental measurements using radiochromic films. The authors concluded that for the case of an implant configuration of 8 seeds spaced 1.5 cm apart in a cubic structure, the gamma index (2%/2 mm) criteria improved from 40.8% to 90.5%.

In Fekete et al. [12], the role played by the presence of heterogeneities in the prostate was discussed. Geant4 MC simulations were made following TG-186 recommendations. Different scenarios were presented including the case of dose to medium in medium as compared to dose to water in medium. The authors concluded that calcifications alter the dose coverage and may result in severe dose perturbation that may require recalculation.

Bonenfant et al. [13] improved the physics library included in bGPUMCD, a MC algorithm executed on Graphics Processing Units, for fast dose calculations in permanent prostate implant dosimetry. For permanent prostate implants, MC-based dosimetric indices were obtained in 30 s with differences within 2.7% with respect to an independent and validated MC code (Geant4).

Pope et al. [14] investigated the effect of prostatic calcifications on brachytherapy treatments by means of MC calculations. Calcification samples were characterized with micro-particle induced X-ray emission to determine their heavy element composition. Clinical brachytherapy treatments were modelled using MC calculations. Dose reductions were observed to be up to 30% locally to the calcification boundary, calcification size dependent. Single large calcifications and closely placed calculi caused local dose reductions of 30% – 60%. Dosimetric parameters like prostate $D_{90}$ showed a reduction of 2% – 5%, regardless of calcification surface area and volume. The parameters $V_{100}$, $V_{150}$ and $V_{200}$ were also reduced by as much as 3% and on average by 1%. It should be noted that Pope et al were not able to reproduce the results reported by Chibani and Williamson.

Miksys et al. [15] have recently published a retrospective study between water-based and full tissue model Monte Carlo dose calculations in a large cohort of patients undergoing I-125 permanent implant prostate brachytherapy. The MC code EGSnrc BrachyDose was employed to analyze 613 patients using two virtual patient models, one TG43-based and one including CT-derived heterogeneous tissue composition and interseed effect. Among other effects, they reported that patients with prostate calcifications can have substantial underdosed volumes due to calcification shielding, lowering the $D_{90}$ value up to 25%.

In 2015, an analytical algorithm designed to account for the presence of calcifications in LDR prostate brachytherapy treatments, RayStretch, was developed by Hueso-Gonzalez et al. [16]. The MC simulations performed there showed a good agreement with the algorithm for the case of a single seed position. Anatomic details from a real patient with calcifications were obtained from a CT image. In this study, we aim to benchmark RayStretch in a real clinical $^{125}I$ seeds prostate implant. Therefore, the main goals of this study are:

1. To benchmark RayStretch against a detailed MC simulation in a realistic clinical case.

2. To evaluate the resilience of RayStretch to accurately estimate dose for two large prostate calcification volumes and three densities. Those configurations are to be considered worst-case scenarios.
3. To measure the calculation time of RayStretch for a realistic implant and voxel grid.
4. To assess the next steps towards the implementation of RayStretch in intraoperative ultrasound planning.

## Materials and Methods

### *RayStretch*

A full discussion on the RayStretch algorithm can be found in Hueso-Gonzalez *et al*. [16]. Nevertheless, for the sake of completeness, we discuss its main characteristics in the following. RayStretch is an algorithm based on the TG-43 formalism [17], able to accommodate the existence of calcifications in the prostate. Therefore, effects like interseed attenuation are not taken into account. To do so, an effective radial dose function $g_{eq}(r)$ is evaluated from the TG-43 consensus radial dose function $g_P(r)$ already incorporated into the TPS. In doing so, minimal modifications in the TPS will be required to implement RayStretch in clinical practice.

The effective radial dose function is evaluated making use of an effective distance constructed assuming that the energy deposited along a path $r_{cal}$ inside a calcification would have been deposited along a longer path $r_{cal,eq}$ in water, *i.e.* if the calcification were absent. Therefore, to define the effective distance $r_{cal,eq} = \lambda\, r_{cal}$, a scaling parameter $\boldsymbol{\lambda = \frac{\mu_{Ca}}{\mu_w}}$ is required, where $\mu$ stands for the linear attenuation coefficient, *Ca* for the calcification and *w* for water. This parameter has to be adjusted empirically by comparing the algorithm with a MC simulation where a particular seed and calcification composition is established beforehand. An empirical value $\boldsymbol{\lambda = 5.3}$ was used in Hueso-Gonzalez *et al*. [16] and in the following. Thus, the simplified recipe for applying the algorithm becomes:

$$\boldsymbol{r_{eq}(r) = r_w + \lambda\, r_{cal}}\,, \tag{1}$$

where $r$ is the real distance between seed and calculation point, $r_w$ is the subsegment of $r$ crossing water and $r_{cal}$ the part inside a calcification. Depending on whether the calculation voxel is inside or outside the calcification, an effective radial dose function can be derived:

$$g_{eq}(r) = \begin{cases} g_w(r_{eq}), & \textbf{voxel in water} \\ \frac{(\mu/\rho)_{cal}}{(\mu/\rho)_w} g_w(r_{eq}), & \textbf{voxel in calcification} \end{cases} \quad (2)$$

where $g_{eq}$ refers to the effective radial dose function and $g_w$ to the TG-43 radial dose function $g_P(r)$ consensus data of the seed considered. See Hueso-Gonzalez *et al*. [16] for a detailed discussion on how the effective radial dose function is evaluated. Thus, RayStretch requires just a minimum modification of the current TG-43 based TPS. It should be noted that voxels are assigned to either water or calcification, whatever is the largest in the voxels. Therefore, no mixed voxels are considered.

The $^{125}$I 6711-OncoSeed™ seed was chosen to create the current working implementation of RayStretch because it was the most widely used worldwide until January 2017. While no longer available, the impact of this work is relevant as there are many seeds whose design is very similar to such model.

To our knowledge, calcification composition is not a subject that has been widely analyzed in the literature. Therefore, in Hueso-Gonzalez *et al*. [16] a standard composition by weight was considered for the calcification: H(5.6%), C(26.5%), N(3.6%), O(40.5%), Na(0.1%), Mg(0.2%), P(7.3%), S(0.3%) and Ca(15.9%). Such composition corresponds to a standard calcium-rich material with Hounsdfield numbers in the range 800-900 [18]. For this particular composition, solid objects have densities of the order of 1.5 g/cm$^3$ (see Fig 9 in Ref. [18]). Therefore, we assumed that as an upper limit for the possible density values. It should be emphasized that RayStretch has not been designed to manage tissue composition differences in the way MC does. Its purpose is to improve LDR implant dosimetry by using modified TG-43 consensus data. Then, its implementation in current TPSs will require simple modifications. In this way it can be used during the implant procedure in clinical practice with minimal effort.

*Clinical Case*

In this work we have applied RayStretch to a clinical LDR prostate implant provided by the University and Polytechnic Hospital La Fe. For this implant 71 6711-OncoSeedTM seeds divided in 15 catheters were used. Their planned source strength was 0.662 U for a total prescribed dose of 160 Gy. It is to note that this prescription dose is in contrast to societal guidelines which recommend a prescription dose of 144/145 Gy [1] [2]. Contouring of all organs as defined by the radiation

oncologist was also included in the plan. The prostate had a volume of 45.2 $cm^3$ and the MC-evaluated prostate $D_{90}$ was 108%. The rectum had a $D_{2cc}$ of 73% and the urethra a $D_{10}$ of 118%. Being a realistic clinical implant, it followed the clinical recommendations established by ESTRO/EAU/EORTC [1] that we briefly summarize here for the sake of completeness: i) The prescribed dose will be in the range 140 Gy – 160 Gy where $D_{90}$ will be in the range 90% – 130%, ii) $D_{2cc}$ in the rectum ≤ 100 % reference prescription dose, and iii) $D_{10}$ in the urethra ≤ 150 % reference prescription dose. According to the Radiation Therapy Oncology Group Protocol 0232 [19], variations of prostate $D_{90}$ in the range 80% – 90% or larger than 130% will be deemed acceptable while values lower than 80% will be considered unacceptable, being considered a Medical Event.

The possibility of using CT images to obtain the mass density of each voxel and to include this information into RayStretch was studied in Hueso-Gonzalez *et al*. [16]. In this work, we have preferred to explore the compliance and robustness of RayStretch in clinical conditions by contouring artificial calcifications in the prostate. Our aim is to benchmark RayStretch performance in worst-case scenarios, where the prostate contains large calcifications in the most probable locations (prostate lobules). Therefore, two different conditions have been explored:

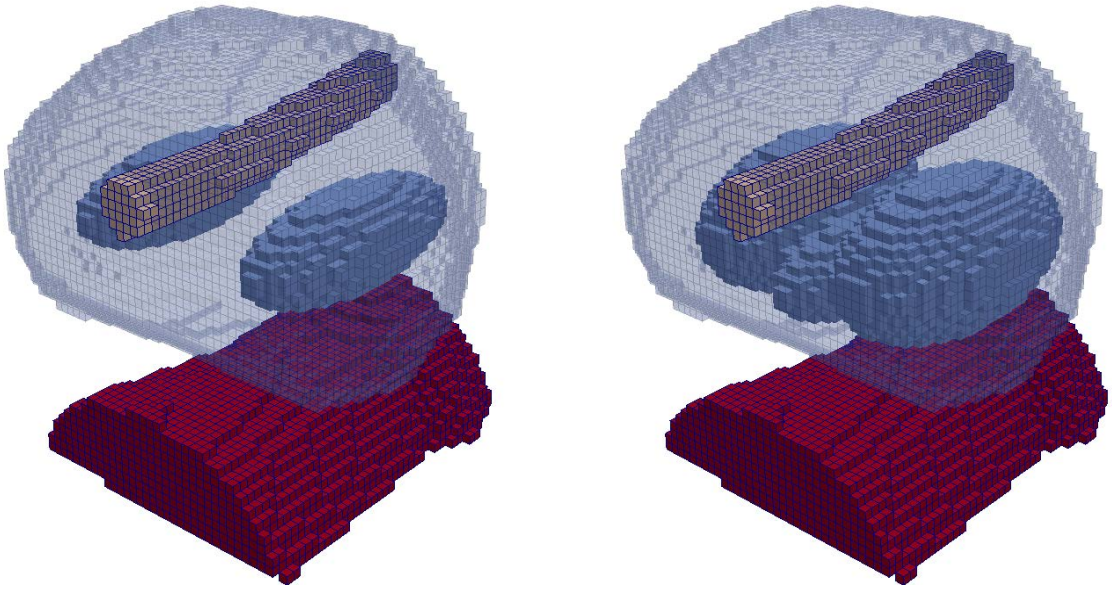

**(a)** **(b)**

**Figure 1.** Figure (a) corresponds to Case A and Figure (b) to Case B. Voxelized reconstruction of the prostate (transparent blue), rectum (red), urethra (brown), and calcifications (blue) volumes. The organ segmentation is based on US planning and the voxels have been determined by a home-made automatic segmentation algorithm as described in the text.

- Case A, Figure 1a, made of two ellipsoidal calcifications, covering 11% of prostate volume, and mainly located in the posterior lobes. This choice is motivated by the frequent localization of calcifications close to the apex in prostate patients.
- Case B, Figure 1b, is formed by three ellipsoidal calcifications, occupying 30% of the target volume, and situated both in the posterior lobes and close to the prostate apex.

Additionally, three mass densities have been chosen for the calcified region, 1.05, 1.20, and 1.35 g/cm$^3$, labeled as I, II and III, respectively. The calcification composition has not been altered in any case. Therefore, 6 different cases (AI, AII, AIII, BI, BII, BIII) ranging from small low density calcifications to large high density ones are explored to test RayStretch even in worst case scenarios.

The extreme cases AIII and BIII are particularly interesting, as the knowledge about inadequate dosimetry inherent to TG-43 in these cases may persuade physicians to not recommend this type of patients for LDR prostate BT. This is the case at the University and Polytechnic Hospital La Fe, where a patient falling into Case BIII will not be considered for LDR brachytherapy treatment due to the presence of such extended calcifications, independently of whether the treatment would be advisable for this tumoral lesion. This patient is then treated using HDR $^{192}$Ir BT in two fractions.

*Monte Carlo simulation*

A comprehensive description of the MC simulation and code are given in Hueso-Gonzalez *et al*. [16], hence we only briefly summarize here its main details. The 6711-OncoSeed™ seed consists of a 4.5 mm welded titanium capsule, 0.05 mm thick, with welded end caps. The capsule contains a 2.8 mm long silver rod onto which $^{125}$I (mixture of AgBr and AgI in a 2.5:1 molecular ratio) is deposited. A full description of its geometry and TG-43 parameters can be found in Dolan et al. [20].

Penelope2008, a MC code whose reliability and performance have been widely tested [21] has been used in this work. Further information on this software can be found elsewhere [22], [23]. Benchmark simulations have been performed comparing the latest Penelope2011 version with respect to the 2008 version used in the following and negligible differences have been observed.

Collisional kerma using home-made routines and absorbed dose have been evaluated in a Cartesian grid of 61×61×46 voxels, each with a volume of 1 mm$^3$, for the six scenarios described above (Case AI to Case BIII) plus TG-43 conditions (water phantom with no calcifications). Since RayStretch does not take into account interseed attenuation, that effect has not been considered in the simulations.

To speed up the simulation, the photon spectrum leaving the encapsulation of a single seed submerged in water was scored and then emitted isotropically from each one of the positions where the TPS positioned a seed. For the total implant $N=10^9$ histories were simulated for each seed (Type A uncertainty of 1.6% ($k$=2) for each seed), that will produce a total statistic of $N=7.1\times10^{10}$ histories and an average Type A uncertainty of 0.2% ($k$=2). This approach allows us to greatly reduce the simulation time at the expense of neglecting dose differences close to the source due to its geometry.

To flag each voxel as belonging to a particular organ at risk (OAR) or the target, a home-made software has been developed to automatically segment the DICOM file for use in RayStretch and the MC calculation. To do so, a voxel is assigned to a given volume when its center is inside the contour. This particular criterion might differ for a given TPS, and therefore some small discrepancies might appear in the case of small organs.

**Results and Discussion**

As explained above, Raystretch makes use of the TG-43 consensus dataset for the 6711 seed. These datasets do not vary much when a different seed model with similar design is chosen, hence no different results are expected for other similar $^{125}$I seeds.

An example of the dose delivered to each voxel in a particular slice of the grid is shown in Figure 2 for the Case AI (small, low density calcifications). As expected, the TG-43 (homogeneous case) does not take into account the effect on the dosimetry caused by the presence of calcified regions. To illustrate the accuracy of RayStretch, we depict in Fig. 2(d) its ratio with respect to MC. Large differences are expected very close to the seed, see discussion below. We show a rebinned histogram using 4 mm × 4 mm voxels. The similarity between RayStretch and the MC simulation is qualitatively visible for the majority of voxels (excluding those close to the seeds, marked as red dots). The same pattern can be found in all slices and cases. On a more quantitative perspective, the Dose-Volume Histogram (DVH) parameters are compared in Figure 3 for the six cases and calculation methods. Values of prostate $D_{90}$, rectum $D_{2cc}$ and urethra $D_{10}$ are also given in Table 1. Differences due to the use of absorbed dose or kerma are less than 0.5% in all cases. In Figure 3 all DVHs listed as TG-43 data correspond to the values given by RayStretch in TG-43 conditions, *i.e.*, unbounded water phantom with no calcifications.

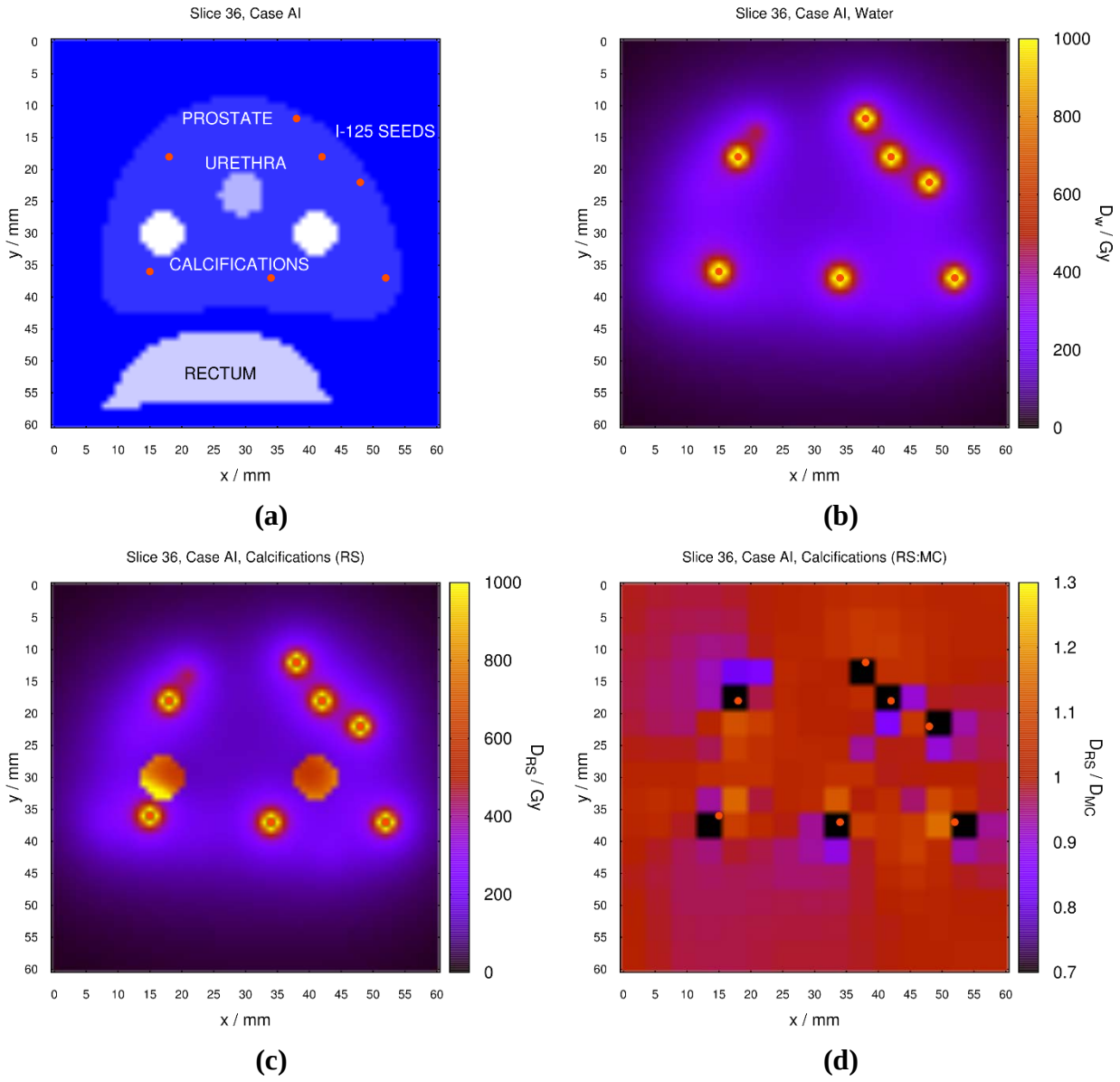


**Figure 2.** (a): Transverse slice of the patient corresponding to Case AI showing the organ segmentation and the actual seed implant. Seeds are depicted as red dots. (b): Dose calculated for this transverse slice using the TG-43 formalism (all water). (c): Same using RayStretch (RS). (d): Dose ratios between RayStretch and MC (2D histogram rebinned to 4 mm × 4 mm voxels to ease visualization).

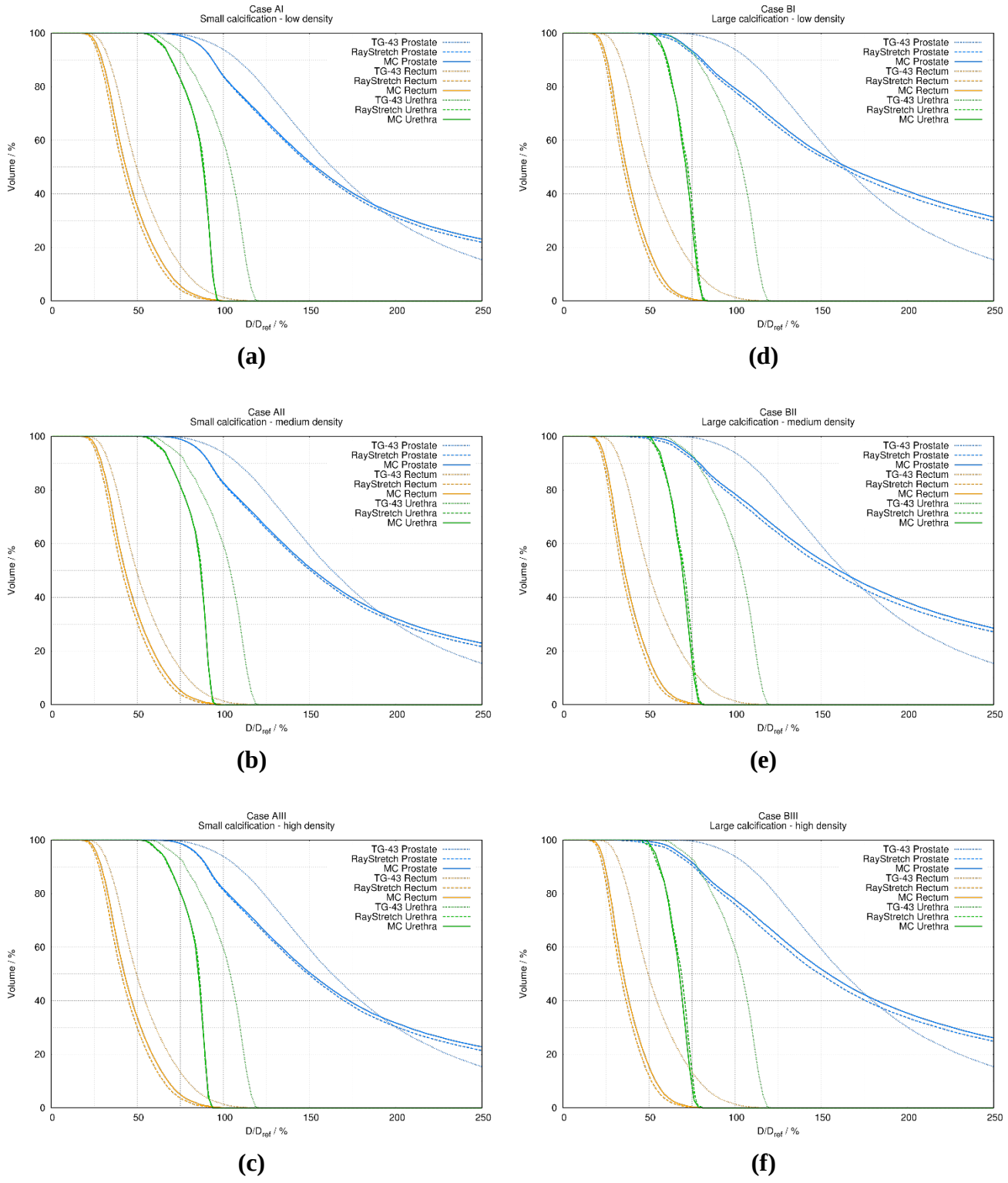


**Figure 3.** DVH for Case A (left panels, small calcification with low (a), medium (b) and high (c) densities) and Case B (right panels, large calcification with low (d), medium (e) and high (f) densities) in TG-43 conditions evaluated using RayStretch, see text for details (dotted line); the MC

calculation (dashed line) and the RayStretch algorithm (solid line) for all three calcification densities and organs: prostate (blue), rectum (orange lines), and urethra (green). $D_{ref}$ stands for the total prescribed dose of 160 Gy.

**Table 1.** Values of prostate $D_{90}$, rectum $D_{2cc}$, and urethra $D_{10}$ (as % of the 160 Gy prescribed dose) for the six cases analyzed (AI to BIII) and also for TG-43 conditions (unbounded water phantom with no calcifications). RS corresponds to the values obtained with RayStretch and MC for the MC calculation.

| | $D_{90}$ Prostate (%) | | $D_{2cc}$ Rectum (%) | | $D_{10}$ Urethra (%) | |
|---|---|---|---|---|---|---|
| Method | RS | 1-RS/MC | RS | 1-RS/MC | RS | 1-RS/MC |
| TG-43 | 110 | 1.8 | 69 | 5.5 | 116 | 1.7 |
| AI | 94 | 0.0 | 61 | 4.7 | 94 | 1.0 |
| AII | 92 | 0.0 | 61 | 3.2 | 93 | 1.1 |
| AIII | 90 | 1.1 | 60 | 4.8 | 90 | 2.2 |
| BI | 80 | 1.2 | 51 | 3.8 | 79 | 1.2 |
| BII | 78 | 1.3 | 49 | 3.9 | 77 | 1.3 |
| BIII | 76 | 2.6 | 48 | 4.0 | 76 | 1.3 |

The prostate $D_{90}$ decreases more than 10 percentage points in all cases with respect to the homogeneous TG-43 case. Some cases (BIII) are low enough to be deemed *unacceptable* by RTOG Protocol 0232 and even flagged as a Medical Event. Prostate $D_{90}$ results given by the full MC calculation agree within an average value of 1.0% (range 0.0% – 2.6%) with the RayStretch algorithm. With respect to rectum $D_{2cc}$, the differences are in the range 3.2% – 4.7%, averaging 4.1%, while for the urethra $D_{10}$ the range becomes 1.0% – 2.2% and its average discrepancy 1.3%. These results allow us to establish a confidence level of 1% – 4% for RayStretch in reproducing a clinical plan.

The main source of these differences can be traced back to two different issues. On one hand, the implementation of the automatic segmentation algorithm chosen might differ from the one used in the MC calculation, especially for those organs close to the DICOM anatomical structure borders or for small ones, hence the numbers of voxels assigned to the organs may vary slightly. On the other hand, seeds positions in MC are exactly those given by the TPS in the planning system. The current implementation of RayStretch rounds this seed position to the center of the closest voxel. Thus, dose discrepancies between RayStrecth and MC are expected in the seed vicinity.

By analyzing a density range of 1.05 g/cm$^3$ to 1.35 g/cm$^3$ and different calcification volumes (10% – 30% of the prostate) one can evaluate the resilience of RayStretch when dealing with different clinical conditions. As it can be observed in Table 1, the quality of the comparison between MC and RayStretch does not degrade when deviating further from TG-43 conditions, either by increasing the density (I→III) or the calcification volume (A→B). This suggests the ability of RayStretch to accurately estimate dose for a variety of clinical situations.

With respect to numerical efficiency, although no expert computing effort has been made to improve RayStretch numerical performance, its present implementation is able to evaluate a full implant in less than 25 seconds on a personal computer. An effort in reducing this computational time to obtain sub-second performance is underway.

Finally, future steps on the road towards clinical translation are:

- To test the robustness of RayStretch with other types of LDR seeds ($^{103}$Pd, $^{131}$Cs).
- To include air cavities as a second type of heterogeneity in the algorithm.
- To perform US-based tissue segmentation (input data for RayStretch). The volumes determined as regions of interest from a CT performed before the implant together with the average electronic densities (obtained from the Hounsfield numbers) have to be registered with real time US images used during the intraoperative procedure. The uncertainty in the determination of the mass density of the calcifications and its effect on the dosimetry have to be investigated.

**Conclusions**

RayStretch is an analytical but robust algorithm for heterogeneity corrections in prostate BT. It has been tested using a realistic clinical prostate $^{125}$I implant including virtual calcifications, benchmarking RayStretch against worst-case scenarios. The results for DVH-related parameters agree with complete MC calculations within an average of 1.0% for prostate $D_{90}$, 4.1% for rectum $D_{2cc}$ and 1.3% for urethra $D_{10}$. This allow us to establish a confidence level of 1% – 4% for RayStretch in reproducing a clinical plan. In contrast to sub-minute MC simulations, RayStretch is based on TG-43 consensus data and simplified tissue segmentation. Thus, it has the potential to be easily implemented in commercial TPSs with minor efforts and software modifications. Its high calculation speed opens up the horizon of dose recalculation in real-time intraoperative treatment planning based on US imaging.

**Acknowledgments**

The authors wish to thank Cristian Candela-Juan for useful discussions. This study was partly supported by a fellowship grant from the Spanish Ministry of Education; by the Generalitat Valenciana [Project PROMETEOII/2013/010]; and by the Spanish Government [Project No. FIS2013-42156].

## References

[1] C. Salembier, P. Lavagnini, P. Nickers, P. Mangili, A. Rijnders, A. Polo, J. Venselaar, and P. Hoskin, "Tumour and target volumes in permanent prostate brachytherapy: A supplement to the ESTRO/EAU/EORTC recommendations on prostate brachytherapy" *Radiother. Oncol.*, vol. 83, no. 1, pp. 3–10, 2007. http://dx.doi.org/10.1016/j.radonc.2007.01.014

[2] B. J. Davis, E. M. Horwitz, W. R. Lee, J. M. Crook, R. G. Stock, G. S. Merrick, W. M. Butler, P. D. Grimm, N. N. Stone, L. Potters, A. L. Zietman, and M. J. Zelefsky, "American Brachytherapy Society consensus guidelines for transrectal ultrasound-guided permanent prostate brachytherapy" *Brachytherapy*, vol. 11, no. 1, pp. 6–19, 2012. https://doi.org/10.1016/j.brachy.2011.07.005

[3] L. Beaulieu, A. Carlsson-Tedgren, J.-F. Carrier, S. D. Davis, F. Mourtada, M. J. Rivard, R. M. Thomson, F. Verhaegen, T. a. Wareing, and J. F. Williamson, "Report of the Task Group 186 on model-based dose calculation methods in brachytherapy beyond the TG-43 formalism: current status and recommendations for clinical implementation." *Med. Phys.*, vol. 39, no. 10, pp. 6208–36, 2012. http://dx.doi.org/10.1118/1.4747264

[4] F. Ballester, A. Carlsson-Tedgren, D. Granero, A. Haworth, F. Mourtada, G. P. P. Fonseca, K. Zourari, P. Papagiannis, M. J. Rivard, F.-A. Siebert, R. S. Sloboda, R. L. Smith, R. M. Thomson, F. Verhaegen, J. Vijande, Y. Ma, and L. Beaulieu, "A generic high-dose rate (192)Ir brachytherapy source for evaluation of model-based dose calculations beyond the TG-43 formalism." *Med. Phys.*, vol. 42, no. 6, pp. 3048–61, Jun. 2015. https://doi.org/10.1118/1.4921020

[5] R. Klimas, B. Bennett, and W. A. Gardner, "Prostatic calculi: A review," *Prostate*, vol. 7, no. 1, pp. 91–96, 1985. http://dx.doi.org/10.1002/pros.2990070110

[6] O. Chibani and J. F. Williamson, "MCPI: a sub-minute Monte Carlo dose calculation engine for prostate implants." *Med. Phys.*, vol. 32, no. 12, pp. 3688–98, Dec. 2005. http://dx.doi.org/10.1118/1.2126822

[7] R. E. P. Taylor, G. Yegin, and D. W. O. Rogers, "Benchmarking BrachyDose: Voxel based EGSnrc Monte Carlo calculations of TG-43 dosimetry parameters." *Med. Phys.*, vol. 34, no. 2,

pp. 445–57, Feb. 2007. http://dx.doi.org/10.1118/1.2400843

[8] J. G. H. Sutherland, R. M. Thomson, and D. W. O. Rogers, “Changes in dose with segmentation of breast tissues in Monte Carlo calculations for low-energy brachytherapy” *Med. Phys.*, vol. 38, no. 8, p. 4858, 2011. http://dx.doi.org/10.1118/1.3613167

[9] J. Sutherland, N. Miksys, P. Soubiran, J. Cygler, and R. Thomson, “SU-E-T-732: The Effects of Calcification Modeling for Monte Carlo Dose Calculations of Low Dose Rate Prostate Brachytherapy” *Med. Phys.*, vol. 42, no. 6, pp. 3505–3505, Jun. 2015. http://www.ncbi.nlm.nih.gov/pubmed/26128394

[10] S. Mashouf, E. Lechtman, L. Beaulieu, F. Verhaegen, B. M. Keller, A. Ravi, and J.-P. Pignol, “A simplified analytical dose calculation algorithm accounting for tissue heterogeneity for low-energy brachytherapy sources.” *Phys. Med. Biol.*, vol. 58, no. 18, pp. 6299–315, Sep. 2013. http://dx.doi.org/10.1088/0031-9155/58/18/6299

[11] S. Mashouf, E. Lechtman, P. Lai, B. M. Keller, A. Karotki, D. J. Beachey, and J. P. Pignol, “Dose heterogeneity correction for low-energy brachytherapy sources using dual-energy CT images.,” *Phys. Med. Biol.*, vol. 59, no. 18, pp. 5305–16, Sep. 2014. http://dx.doi.org/10.1088/0031-9155/59/18/5305

[12] C. A. Collins Fekete, M. Plamondon, A. G. Martin, É. Vigneault, F. Verhaegen, and L. Beaulieu, “Calcifications in low-dose rate prostate seed brachytherapy treatment: Post-planning dosimetry and predictive factors” *Radiother. Oncol.*, vol. 114, no. 3, pp. 339–344, 2015. http://dx.doi.org/10.1016/j.radonc.2015.01.014

[13] É. Bonenfant, V. Magnoux, S. Hissoiny, B. Ozell, L. Beaulieu, and P. Després, “Fast GPU-based Monte Carlo simulations for LDR prostate brachytherapy” *Phys. Med. Biol.*, vol. 60, no. 13, pp. 4973–4986, 2015. http://dx.doi.org/10.1088/0031-9155/60/13/4973

[14] D. J. Pope, D. L. Cutajar, S. P. George, S. Guatelli, J. A. Bucci, K. E. Enari, S. Miller, R. Siegele, and A. B. Rosenfeld, “The investigation of prostatic calcifications using μ-PIXE analysis and their dosimetric effect in low dose rate brachytherapy treatments using Geant4.” *Phys. Med. Biol.*, vol. 60, no. 11, pp. 4335–4353, 2015. http://dx.doi.org/10.1088/0031-9155/60/11/4335

[15] N. Miksys, E. Vigneault, A.-G. Martin, L. Beaulieu, and R. M. Thomson, “Large-scale Retrospective Monte Carlo Dosimetric Study for Permanent Implant Prostate Brachytherapy” *Int. J. Radiat. Oncol.*, vol. 97, no. 3, pp. 606–615, 2017. http://dx.doi.org/10.1016/j.ijrobp.2016.11.025

[16] F. Hueso-González, J. Vijande, F. Ballester, J. Perez-Calatayud, and F.-A. Siebert, “A simple analytical method for heterogeneity corrections in low dose rate prostate brachytherapy.”

*Phys. Med. Biol.*, vol. 60, no. 14, pp. 5455–69, Jul. 2015. http://dx.doi.org/10.1088/0031-9155/60/14/5455

[17] M. J. Rivard, B. M. Coursey, L. A. DeWerd, W. F. Hanson, M. S. Huq, G. S. Ibbott, M. G. Mitch, R. Nath, and J. F. Williamson, "Update of AAPM Task Group No. 43 Report: A revised AAPM protocol for brachytherapy dose calculations." *Med. Phys.*, vol. 31, no. 3, pp. 633–674, 2004. http://dx.doi.org/10.1118/1.1646040

[18] W. Schneider, T. Bortfeld, and W. Schlegel, "Correlation between CT numbers and tissue parameters needed for Monte Carlo simulations of clinical dose distributions" *Phys. Med. Biol.*, vol. 45, no. 2, pp. 459–478, 2000. http://dx.doi.org/10.1088/0031-9155/45/2/314

[19] B.R. Prestidge, "Radiation Therapy Oncology Group (RTOG): Protocol 0232: a phase III study comparing combined external beam radiation and transperineal interstitial permanent brachytherapy with brachytherapy alone for selected patients with intermediate-risk prostatic car.". https://www.rtog.org/ClinicalTrials/ProtocolTable/StudyDetails.aspx?study=0232. [Accessed: 25-Jul-2016].

[20] J. Dolan, Z. Li, and J. F. Williamson, "Monte Carlo and experimental dosimetry of an 1251 brachytherapy seed." *Med. Phys.*, vol. 33, no. 12, pp. 4675–84, Dec. 2006. http://dx.doi.org/10.1118/1.2388158

[21] S.-J. Ye, I. A. Brezovich, P. Pareek, and S. A. Naqvi, "Benchmark of PENELOPE code for low-energy photon transport: dose comparisons with MCNP4 and EGS4" *Phys. Med. Biol.*, vol. 49, no. 3, pp. 387–397, Feb. 2004. http://dx.doi.org/10.1088/0031-9155/49/3/003

[22] J. Sempau, A. Badal, and L. Brualla, "A PENELOPE-based system for the automated Monte Carlo simulation of clinacs and voxelized geometries-application to far-from-axis fields." *Med. Phys.*, vol. 38, no. 11, pp. 5887–95, Nov. 2011. http://dx.doi.org/10.1118/1.3643029

[23] F. Salvat, "PENELOPE-2014: A Code System for Monte Carlo Simulation of Electron and Photon Transport", (Issy-Les-Moulineaux: OECD Nuclear Energy Agency). https://www.oecd-nea.org/dbprog/courses/nsc-doc2015-3.pdf.